OXFORD

Cerebral Cortex, 2023, 1–16
https://doi.org/10.1093/cercor/bhad003
Original Article

Persuader-receiver neural coupling underlies persuasive messaging and predicts persuasion outcome

Yangzhuo Li [1], Xiaoxiao Luo[2], Keying Wang[2], Xianchun Li [1,3,4,*]

[1]Shanghai Key Laboratory of Mental Health and Psychological Crisis Intervention, Affiliated Mental Health Center (ECNU), School of Psychology and Cognitive Science, East China Normal University, Shanghai 200062, China,
[2]Shanghai Key Laboratory of Mental Health and Psychological Crisis Intervention, School of Psychology and Cognitive Science, East China Normal University, Shanghai 200062, China,
[3]Shanghai Changning Mental Health Center, Shanghai 200062, China,
[4]Institute of Wisdom in China, East China Normal University, Shanghai 200062, China

*Address correspondence to Xianchun Li. Email: xcli@psy.ecnu.edu.cn

Opportunities to persuade and be persuaded are ubiquitous. What interpersonal neural pathway in real-world settings determining successful information propagation in naturalistic two-person persuasion scenarios? Hereby, we extended prior research on a naturalistic dyadic persuasion paradigm (NDP) using dual-fNIRS protocol simultaneously measured the neural activity from persuader-receiver dyads while they engaged in a modified "Arctic Survival Task." Investigating whether neural coupling between persuaders and receivers underpinning of persuading and predict persuasion outcomes (i.e., receiver's compliance). Broadly, we indicated that the persuasive arguments increase neural coupling significantly compared to non-persuasive arguments in the left superior temporal gyrus-superior frontal gyrus and superior frontal gyrus-inferior frontal gyrus. G-causality indices further revealed the coupling directionality of information flows between the persuader and receiver. Critically, the neural coupling could be a better predictor of persuasion outcomes relative to traditional self-report measures. Eventually, temporal dynamics neural coupling incorporating video recording revealed neural coupling marked the micro-level processes in response to persuading messages and possibly reflecting the time that persuasion might occurs. The initial case of the arguments with targeted views is valuable as the first step in encouraging the receiver's compliance. Our investigation represented an innovative interpersonal approach toward comprehending the neuroscience and psychology underlying complex and true persuasion.

Key words: persuasion; naturalistic dyadic persuasion paradigm (NDP); dual-FNIRS protocolneural coupling.

Introduction

Persuasion may be unique to *Homo sapiens*, which refers to the active attempt or intention by an individual, or group (i.e., "persuaders") to alter the convictions, attitudes, or behaviors of targets of persuasion (i.e., "receivers") by diverse communicative implications, is practiced widely in diverse fields including psychology, sociology, communications, health, political science, marketing, as well as economics (Cascio et al. 2015; Shteynberg et al. 2016; Humă et al. 2020). Real-world persuasion often involves multiple people in conversation, various connections between persuasive message producer and receiver. Whereas substantial research has been conducted on the neural correlates of persuasion production, the interpersonal neural pathways that translate messages into effects on individuals and populations are not fully comprehended, thus offering limited insight into the brain systems underlying persuasion during the naturalistic interaction (Hari et al. 2015; Redcay and Schilbach 2019).

In traditional individual neuroimaging studies, neurocognitive mechanisms underlying persuasion were investigated from the receiver's perspective and the persuader's perspective, correspondingly. A growing body of research has described how information becomes ingrained in the brains of recipients (for review see Cascio et al. 2015), highlighting the prominent role of the value system (i.e., ventromedial prefrontal cortex, medial prefrontal cortex, ventral striatum) (see Cacioppo et al. 2018; Falk and Scholz 2018 for reviews; Falk et al. 2010, 2011, 2015) and mentalizing system (i.e., dorsomedial prefrontal cortex, precuneus, temporoparietal junction). Specifically, the value system may represent the integration of the message's value into the receiver's self-concept and as a central predictor of whether persuasive messages will be effective in altering behavior, including smoking cessation (Cooper et al. 2015; Riddle Jr et al. 2016), increased sunscreen use (Falk et al. 2010; Vezich et al. 2017) and decreased sedentary behavior (Falk et al. 2015; Cooper et al. 2017). Furthermore, greater activity in the mentalizing system help to make sense of others' opinions and is associated with a greater likelihood of updating recommendations to conform to others (Cascio et al. 2015; Rimal and Lapinski 2015).

Likewise, neuroscientists consider the perspective of the persuader. Existing studies highlight that self-relevance (i.e., the subregions of the medial prefrontal cortex, and posterior cingulate cortex) as well as social relevance (i.e., the brain's mentalizing system, right superior temporal sulcus) are two primary inputs to determining sharing (see Falk and Scholz 2018 for reviews). Greater activity in brain regions implicated in self-relevance increases in response to the ideas that persuaders report wanting to share with others (Falk et al. 2013). Moreover, activity in the mentalizing system linked to the successful

Received: October 5, 2022. **Revised:** December 25, 2022. **Accepted:** December 29, 2023

information propagation. Persuaders who exhibit higher engagement of the brain's mentalizing system particularly within TPJ are more likely to be successful influencers (Dietvorst et al. 2009; Cascio et al. 2015). Individuals who are more able to spread their own views to others produced greater mentalizing activity even during initial encoding ideas (Baek et al. 2017).

Existing neuroimaging paradigms have typically examined persuasion-related neural mechanisms by measuring the brains of isolated individuals, yet, failing to capture the dynamic and bi-directional characteristics of the persuader and receiver from an interpersonal neuroscience perspective. Researchers proposed that when incoming information influences receiver, they are more likely to modify their attitudes and conduct to align with the message producer (Falk and Scholz 2018). Likewise, brains would also provide an efficient path to understanding persuaders and receivers adopting action, which allows them to demonstrate greater cognitive, affective, and behavioral similarity (Iacoboni 2009).

Emerging evidence suggests that biological coupling between persuader and receiver may be a crucial component of effective persuasion, beyond the brain activity observed in either party alone (Scholz et al. 2017; Falk and Scholz 2018). Common neural responses appear to be a hallmark of successful communication and a shared sense of reality within a social group (Schippers et al. 2010; Jiang et al. 2012, 2015; Spunt et al. 2015; Salazar et al. 2021; Hirsch et al. 2021; Holroyd 2022). More recent research demonstrates that stronger messages (i.e., more persuasive versus less persuasive) elicited greater coupling across the brains of audiences, revealing more effective or powerful messages resonate with their target audiences and drive synchronization in brains (Dmochowski et al. 2014; Schmälzle et al. 2015; Imhof et al. 2020). Hence, capturing the similarities across the brains of the persuader and receiver may provide a promising tool for objectively quantifying the impact of persuading on both the persuader and the recipient.

At the meantime, persuading is not a singular event, instead, involves progression through a sequence of distinct stages. For instance, Aquino et al. (2020) defined the cognitive-attitude-change process of persuading that the spread of information (which includes ideas, opinions, and behavior) involves two significant processes: during the initial exposure, people start to implicitly think about the content of the incoming message. During the evaluation, individuals reflect on the self-relevance of the message and express their attitude explicitly. Consequently, a finer resolution of the time dynamics of neural coupling during persuading might add to the understanding of such complex social interactions. As different levels of interpersonal verbal communication may associated with different patterns of neural coupling, based not only on the spatial patterns of neural coupling but also on the temporal patterns of neural coupling (Jiang et al., 2021). We infer each stage of the persuasive messaging process might also presumed to correspond to distinct spatial and temporal neural coupling patterns.

In this paper, we highlight that, in the context of naturalistic dyadic persuasion, neural coupling between the persuader and receiver may facilitate the propagation of specific persuasive signals and, consequently, the modification of preferences or behaviors. This proposition allowed us to test the following relevant hypotheses: (1) The persuader-receiver neural coupling can robustly differentiate the arguments that persuaded the receiver and did not, as persuasive arguments (PA) may induce higher neural coupling than no-persuasive arguments (NPA); (2) considering "brain-as-predictor," the degree of neural coupling could predict eventually persuasion outcomes; and (3) the dynamic neural coupling can continuously track dynamic persuading throughout ongoing arguments messaging and thus might serve as an implicit predictor of where persuasion takes hold.

To address above questions, we developed a naturalistic dyadic persuasion paradigm (NDP) inspired by Jensen (1973), where participants unfold persuading on the basis of an "Arctic Survival Task" scene. Functional near-infrared spectroscopy (fNIRS) was adapted to simultaneously record brain signals from participant dyads. Moreover, fNIRS provides a noninvasive measure of changes in blood oxygenation resulting from neural activity whereas being minimally sensitive to motion artifacts in comparison with EEG or fMRI, enabling the creation of experimental paradigms that more closely resemble real-world situations than classic studies (Jiang et al. 2012, 2015; Boas et al. 2014; García and Ibáñez 2014; Pinti et al. 2017, 2019; Yang et al. 2020). We focused on the prefrontal and left temporo-parietal regions, which are critical brain regions for persuasion (Burns et al. 2018, 2019; Falk and Scholz 2018). Furthermore, the prefrontal constitutes social interactions and decision-making (Pan et al. 2020; Cheng et al. 2022), and the left temporo-parietal regions contribute to social mentalizing (Jiang et al. 2015) and simultaneous natural speech-processing for successful oral communication (Stephens et al. 2010; Dai et al. 2018; Hirsch et al. 2021).

Ethics

The experimental protocol was approved by Human Research Protection Committee at East China Normal University (Number HR 019–2020). Before the study, all procedures were explained to the participants and carried out in accordance with ethical standards. Participants gave written informed consent and were free to leave the experiment at any time.

Materials and methods

Participants

Initially, female–female dyads and male–male dyads were both recruited in our experiment. Nonetheless, we found a gender effect in that male participants are largely immune to the arguments compared to female participants (3 out of 4 male–male dyads were completely unpersuaded, 1 male dyad was persuaded to a low degree). Instead, only 1 out of 4 female–female dyads were completely unpersuaded, while the other three were persuaded to varying degrees). Intending to minimize the sexually dimorphic effects of the current experiment, we merely recruited female–female dyads in subsequent sample collecting. Initial 4 female–female dyads were retained in the sample.

Later, 18 females were excluded for failing to complete two visits (which cannot return to the laboratory for the second visit or experimenters cannot find a suitable match, within the allotted period interval). Besides, one dyad was excluded due to experimenter error and one dyad was excluded due to equipment malfunction or insufficient fNIRS data quality in the scanning session. These resulted in a final sample of 26 dyads (52 healthy, right-handed females, range = 18–30 years, mean ± s.d. = 23.04 ± 2.48 years). Members of each dyad were strangers since the communication behaviors of strangers are determined by a set of communication rules or norms and are unlikely to be influenced by social variables (such as interpersonal closeness, and social ranking) (Jiang et al. 2015; Hirsch et al. 2021). All participants had a normal hearing, normal or corrected-to-normal vision, and no history of neurological,

major medical, or psychiatric diagnosis. None of the participants were currently using psychiatric medication or illegal drugs, nor were they pregnant or breastfeeding.

Materials and experimental procedures

Materials

We test the naturalistic dyadic persuasion (NDP) using the "Arctic Survival Task," a classic experimental paradigm developed by Jensen (1973) where participants rank the importance of a set of salvaged items (e.g., 15 items that conceivably aids a person stranded in a wintery plane crash scenario, see Supplementary "Task descriptions and scoring" for detailed description). This task was selected with care because it elicited a high level of participant engagement and includes a quantifiable measure of the receiver's behavior compliance. Above all else, we considered it was likely to avoid extreme initial attitudes among our participants to leave room for the change. This paradigm was modified in two ways: First, rather than ranking all 15 items according to importance, we asked participants to a limited number of items to select (the three most important items). Therefore, participants must determine the three most important items to hold based on their own opinions and rank order them (i.e., first important item, second important item, and third important item). Second, rather than calculating the correlation between the persuader's initial ranking and the receiver's final ranking (Setlock et al. 2004; Kilduff and Galinsky 2013), the persuasion outcomes were quantified by the amount that the receiver changed their items to match the items of the persuader. These modifications ensured the matched participants in Visit-2 were dissonant at the initial selection and thus facilitated distinguishing persuasion or not. All of these changes were authorized by the ethical review boards.

Experimental procedures

The experiment was conducted over the course of two laboratory visits, i.e., pre-persuading behavioral task (Visit-1) and dual-fNIRS scanning task (Visit-2) (Fig. 1A). During Visit-1, participants arrived independently and provided socio-demographic information (age and education) as well as gave informed consent to take part. Subsequently, they completed a pre-persuading behavioral task (~10 min) assessing their initial items selection in the "Arctic Survival Task" and confidence rating (how confident in selecting, write a number from 0 to 100%). Post-behavioral assessment to regard the involvement, familiarity, and relevant experience to the task scenario, on a scale from 1 to 7 (see Subjective Assessment). For the purpose of minimizing fluctuating effects, after the initial selection, the experimenter reconfirmed the choices of participants to ensure they would not readily alter their decisions in the short term. After receiving an affirmative reply, participants were permitted to leave the lab, and they were instructed not to be concerned about this task before the next visit. Twice visits spaced by no more than 48 h.

Two participants whose initial selections were dissonant were invited to return to the lab at the same time for the dual-fNIRS scanning task (Visit-2). Upon arrival, participants completed the pre-scanning assessment in private and were subsequently randomly assigned to "persuader" or "receiver." No significant differences between the persuader and receiver within each dyad on questionnaires of demographic information, confidence rating, and post-behavioral assessment in Visit-1 ($-0.51 < ts < 1.62$, $ps > 0.1$, paired-sample t-test, two-sided. See Supplementary Table S1), indicated that random assignment of roles was successful. The persuader was instructed to transmit the items and their arguments to the receiver; the receiver got oral arguments from the persuader to determine whether to replace their initial selections with the alternatives. To note, receiver silence was required throughout scanning. The main advantage of this methodology (Dyads were not allowed to actively participate in discussing.) was that it maintains experimental control and facilitates comparison persuaded or not, enabling us to identify how and where persuasion occurs without the potential confounding effect of individual responses. (Anders et al. 2020).

An initial 2-min resting phase was conducted to allow the imaging instrument and participants to reach a steady state. During this phase, participants were instructed to close their eyes, refrain from moving, and relax their minds (Jiang et al. 2015; Zhu et al. 2021). The persuading phase immediately followed the resting phase, persuader made their arguments for which salvaged items they think to be kept to the receiver, face-to-face. Each item was offered for a limited time (~90 s), and audible beeps indicated the start of the speech and the end of the speech. After each item, additional 15 s for the receiver to evaluate from "Concreteness," "Amusement," and "Convincement" on a 9-point scale. After all three items finish, the receiver made the second selection and confidence rating, individually. Receivers were told by the experimenter that their second selection was limited in the items by their initial selection and by the persuader's selection. Finally, the persuader and receiver were administered a series of post-scanning assessments (see *Subjective Assessment*).

A curtain was drawn between the participants and the experimenter, who remained in the room but did not have any contact with the participants and could not be seen by them at any time during the experiment. The entire experiment was video recorded, and the persuader and receiver chairs were slightly oriented toward the camera to enhance whole-body visibility (resulting in approximately a 90–110° angle in between the two chairs' orientations, Fig. 1C).

Behavior data acquisition and processing

Persuading performance assessment

PA and NPA assessment

PA and NPA were differentiated by persuader's items selected by the receiver or not, in the second selection session. Specifically, in each dyad, two changed items averaged as PA and one no-changed item as NPA or one changed item as PA and two no-changed items averaged as NPA. Remarkably, this operation led to 5 dyads being further excluded, of which 2 dyads were unpersuaded (zero items changed) and 3dyads completely persuaded (three items changed). Ultimately, 21 dyads were retained in the final results.

Persuasion outcomes assessment

Persuasion outcomes were measured by the amount of receiver-changed items to match the persuader. Notably, considering the re-ranking order of items could be taken into account as higher persuasiveness for the items placed in the first position than second or third position, we weighed the persuasion outcomes by the persuader initial ranking order and the second-ranking order of items of receiver. In particular, we assigned the values "3," "2," and "1" to the first, second, and third items of the persuader. Values are maintained if the item is in the same order, or values increased or decreased by adding or minus the weighted proportion on the basis of the order (3/6 first item, 2/6 second item, 1/6 third item); the items did not select given "0" value. For example, the receiver put the first item in the second position, the values of $(3-(3/6)\times 1)=2.5$ given; the receiver put the third item in the first position, the values of $(1+(1/6)\times 2)=1.33$ given. Consequently, the outcomes of persuasion determined by the

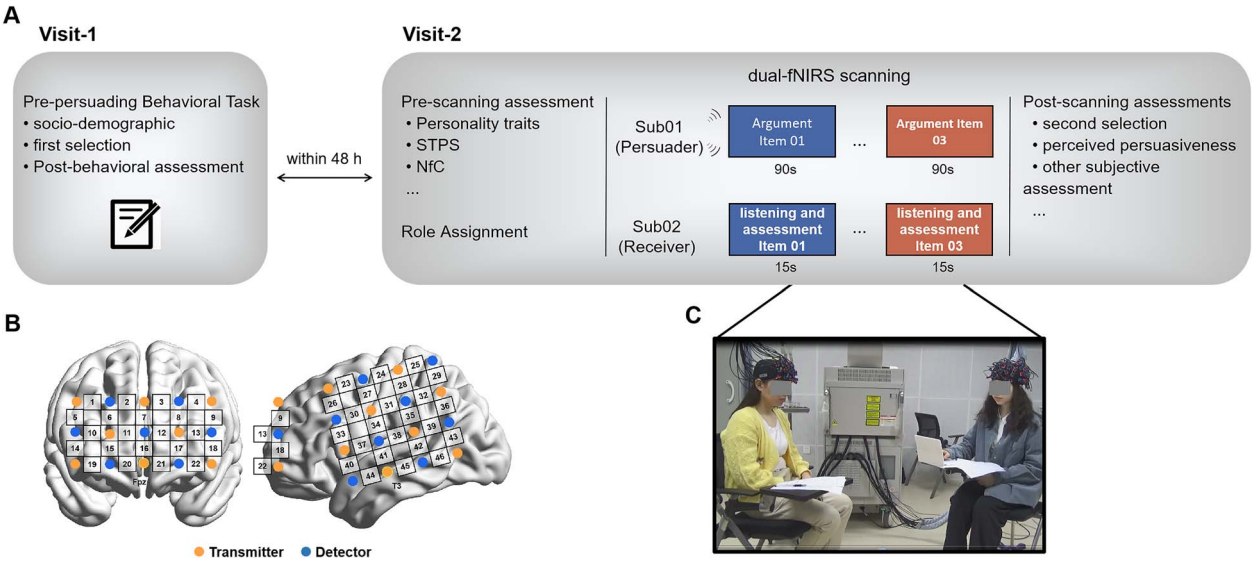

Fig. 1. Experimental protocol. (A) Schematic of the experimental protocol. Participants came to the laboratory for an initial pre-persuading behavioral task (Visit-1), during which they completed the initial task as well as several subjective assessments. Moreover, the dual-fNIRS scanning (Visit-2) took place approximately 1–2 days later and participants were randomly assigned to the "persuader" or "receiver" at this processing to complete the NDP task. (B) fNIRS probe positions. The transmitter (orange circles) and detector (blue circles) are located in the prefrontal and left temporo-parietal areas (inter-optode distance of 30 mm), respectively. The frames that connect the sources and detectors and the numbers shown in black represent the measurement channels (CH). 3 × 5: the middle optode of the lowest probe row of the patch was placed at Fpz, following the international 10–20 system. The middle probe set columns were placed along the sagittal reference curve. 4 × 4: the lowest probe was aligned with the sagittal reference curve, referenced at T3, following the international 10–20 system. All optode probe sets were positioned employing individually sized caps, which enhances the consistency of the signals across variations in head size. (C) Demonstrated here is a snapshot of the dual-fNIRS scanning session.

sum of weighted values, range from 0 to 6. For the effectiveness of weighted persuasion, outcomes see Supplementary "Weighted persuasion outcomes scoring" for detailed descriptions.

To rule out the oral outputs differences potentially could explain the persuading effects, we also conducted validated measures. Specifically, sentences/frequency, word numbers, information richness, and emotional states of each item of each persuader were collection. Sentences/frequency and word numbers are obtained by counting the total numbers, information richness and emotional states are obtained by 9-point scale (1 denotes very rarely, 9 denotes very much). Then, outliers were identified by calculating an interval spanning (via Mahalanobis distance) over the mean 3 ± SD to estimate the variability of these characteristic within dyads; a series of paired sample *t*-tests (two-sided) were conducted to clarity the differences between PA and NPA on these characteristics; a series of correlation analyses (Pearson's correlations, two-sided) between these characteristics and persuasion outcomes. The findings have ruled out the possible confounding of the persuading performance that we observed (see Supplementary "Oral outputs variables" for details).

Subjective assessment

Post-behavioral assessment

This scale contained 7 items: (1) Are you interested in this task scenario? (2) Do you think you are a real member of this scene in doing the task given? (3) How tense or critical is the situation? (4) How familiar are you being with this scenario topic? (5) Have you ever possessed any previous experience with outdoor survival skills (i.e., Trek camping, mountain climbing, field orientation, parachute gliding? (6) Have you seen a survival TV program before, how frequently? (7) Do these experiences aid you in accomplishing the task? (1) ~ (3) for scenario involving and (4) ~ (7) for scenario familiarity and relevant experience, on a 7-point scale (1 denotes very rarely, 7 denotes very frequently).

Pre- and post-scanning assessment

Pre-scanning assessment

In persuader, personality traits (assessed by *Ten Item Personality Inventory*, TIPI. Gosling et al. 2003, Cronbach's $\alpha = 0.82$) and empathy level (assessed by *Interpersonal Reactivity Index* 22-item, IRI. Furthermore, Davis 1983, Cronbach's $\alpha = 0.85$) were measured as these variables affected persuasion in previous literature (Matz et al. 2017; Falk and Scholz 2018; Wall et al. 2019). In the receiver, in addition to personality and empathy level evaluation, the susceptibility to persuasion–as an interindividual variability affects compliance–measured by the *Susceptibility to Persuasion Scale* (STPS, 32-itmes, Modic et al. 2018, Cronbach's $\alpha = 0.84$) and *Need for Consistency scale* (NfC, 18-items, Cacioppo et al. 1984; Cronbach's $\alpha = 0.80$). The participants rated these scales on a 7-point scale. (1 extremely uncharacteristic of me; 7 extremely characteristic of me).

Post-scanning assessment

The persuaders and receivers also completed post-scanning questionnaires. Persuaders evaluated (1) self-presentation (involvement, effort); (2) persuasion strategies employed (warmth, competence, robust arguments); and (3) persuade perception (one's evaluation about the influence on another. 11-point rating ranging from 0 to 100%). Receivers evaluated employing the questionnaire adapted from Zanbaka et al. (2006), insisted on utilizing three criteria to evaluate the persuader: (1) perception of persuader (unfriendly–friendly, incompetent–competent, untrustworthy–trustworthy); (2) oral expression (disorganized–organized, speech rate slow–fast, pitch low–high); (3) facial expression and body language (inexpressively–expressively, unnaturally–naturally); and (4) persuaded perception (one's

evaluation about to be influenced by another), an 11-point rating from 0 to 100%.

fNIRS data acquisition and preprocessing

fNIRS data recording

The dyads' brain activity was simultaneously recorded during Visit-2 scanning using an ETG-7100 optical topography system (Hitachi Medical Corporation, Japan). The optical data were collected with a sampling rate of 10 Hz at wavelengths of 695 and 830 nm. The probes were placed over bilateral frontal and left temporoparietal areas. Particularly, two optode probes were used for each participant 3 × 5 probe covering prefrontal areas (eight transmitters and seven detectors resulting in 22 measurement channels, i.e., CH1–22) and a 4 × 4 probe covering left temporoparietal areas (eight transmitters and eight detectors resulting in 24 measurement channels, i.e., CH23–46), see Fig. 1B for the reference and channel locations. Checking and adjusting the probe set positions across all dyads to ensure uniformity across all participants before the scanning start. The correspondence between the fNIRS channels and the measured points on the cerebral cortex was determined using a virtual registration approach (Singh et al. 2005; Tsuzuki et al. 2007), the anatomical locations and the atlas-based are listed in Supplementary Table S5.

fNIRS data preprocessing

Raw optical intensity signals were first converted into optical density (OD) and visually inspected to assess the signals' quality. Channels showing detector saturation or poor optical coupling as marked by a lack of the heartbeat frequency (~1 Hz) in the signal's power spectrum were removed (Erdoğan et al. 2014; Pinti et al. 2019), which resulted in 98.4% of channels were saving in further analyses. Subsequently, the filtered OD data were converted into oxyhemoglobin (HbO) and deoxyhemoglobin (HbR) concentration changes on the basis of the modified Beer–Lambert Law (Cope and Delpy 1988). During preprocessing, a band-pass second-order Butterworth filter with cut-off frequencies of 0.01–1 Hz was applied to reduce the slow drift and high-frequency noise (Dai et al. 2018; Zhu et al. 2021). We employed a wavelet-based denoising algorithm to further eliminate motion artifacts and global physiological noise (Duan et al. 2018). Specifically, we utilized wavelet transform coherence to automatically detect the time-frequency points per channel that were contaminated by global physiological noise. Then, we decomposed the fNIRS signal using the wavelet transform and suppressed the wavelet energy of the contaminated time-frequency points.

As underlined by previous fNIRS-based two-person neuroscience literature (Jiang et al. 2012, 2015; Dai et al. 2018; Yang et al. 2020; Zhu et al. 2021; Li et al. 2022), HbO more sensitive to changes in the regional cerebral blood flow with higher signal-to-noise ratio, increases in HbO values have been recognized as the consequence of neural activity and corresponds with the blood oxygenation level-dependent signal measured by fMRI (Huppert et al. 2006; Hoshi 2007). Statistical analyses mainly focused on HbO values in the current study. Despite this, HbR values were extracted and tested using the same approach as HbO values (see Supplementary "*HbR analyses results*" for detailed descriptions).

fNIRS data analysis

Neural coupling signatures

A wavelet transforms coherence (WTC) algorithm, which estimates the cross-correlation of two HbO time series in each dyad and each channel combination (CHs) as a function of frequency and time, was used to compute neural coupling between persuader and receiver (Grinsted et al. 2004; Chang and Glover 2010). WTC can reveal a locally phase-locked behavior that may not be uncovered by traditional time series analysis such as Pearson's correlation (Grinsted et al. 2004). WTC values range from 0 (totally unsynchronized) to +1 (perfectly synchronized). These data generated a 2D (time × frequency) matrix of the coherence values. All possible CHs were examined (46 channels from the persuader × 46 channels from the receiver, 2116 CHs in total). Finally, the coherence values were time averaged across the persuasion phase and then converted into Fisher-Z values to generate a normal distribution, as in previous research (same as Dai et al. 2018; Pan et al. 2020, 2021; Li et al. 2022).

Determining the frequencies of interest

We according to the method described in Southgate et al. (2014) to search for frequencies that were most robustly specific to task-related activity (i.e., persuading phase). To accomplish this, coherence values above 0.8 Hz and below 0.01 Hz were excluded to prevent the aliasing of high-frequency physiological noise, such as cardiac activity (0.8–2.5 Hz), extremely low-frequency fluctuations. (Dai et al. 2018; Zhu et al. 2021). Subsequently, coherence values were averaged across CHs in each dyad, this method is unbiased way as we did not have a priori hypotheses for specific CHs of interest (same as Pan et al. 2020, 2021). We conducted a non-parametric permutation procedure on the basis of phase-randomized surrogate data on persuading phase HbO (Maris and Oostenveld 2007; Simony et al. 2016). This method is generated by randomly Fourier-scrambling the original signals, thereby preserving the frequency content of the signals while disrupting their temporal structure (Kingsbury et al. 2019). The permutation procedure was repeated 2000 times to generate a null distribution of CHs averaged pseudo-dyad coherence values at each frequency band. Ultimately, coherence values from the original dyads were in comparison with the null distribution for each frequency band. This analysis yielded a series of *P*-values and corrected adopting false discovery rate (FDR) to control for type I errors (Benjamini and Hochberg 1995) (threshold: *P*-value < 0.05, marked with asterisks. see Fig. 2A). Neighboring frequency bins with a corrected *P*-value below 0.05 were combined into clusters.

Based on above rationale, frequency ranges of interest (FOIs), that is, 0.030–0.048 Hz (22–33 s) were obtained (Fig. 2A). This frequency band did not contain high- or low-frequency noise or Mayer waves (~0.1 Hz, typically between 0.07 and 0.13 Hz), all of which might lead to artificial coherence. Hence, the coherence values within this FOIs were clustered for further analysis.

Neural coupling in PA compared to NPA

In accordance with our hypotheses, we expected higher persuader-receiver neural coupling among PA relative to NPA (PA vs NPA). For purposes of this, we contrasted neural coupling between PA and NPA employing a series of paired sample *t*-tests (two-sided) at all CHs, the resulting *P*-values were corrected by adopting the FDR method to control for type I errors (Benjamini and Hochberg 1995).

Validation analyses on neural coupling

We conducted two validation tests on the significant CHs as a control for non-social effects (Kingsbury et al. 2019; Ayrolles et al. 2021). First, shuffled-items HbO signals within the same dyad (i.e., the HbO signals of Item01 from persuader #1 were repaired with those from Item02 from receiver #1). This operation

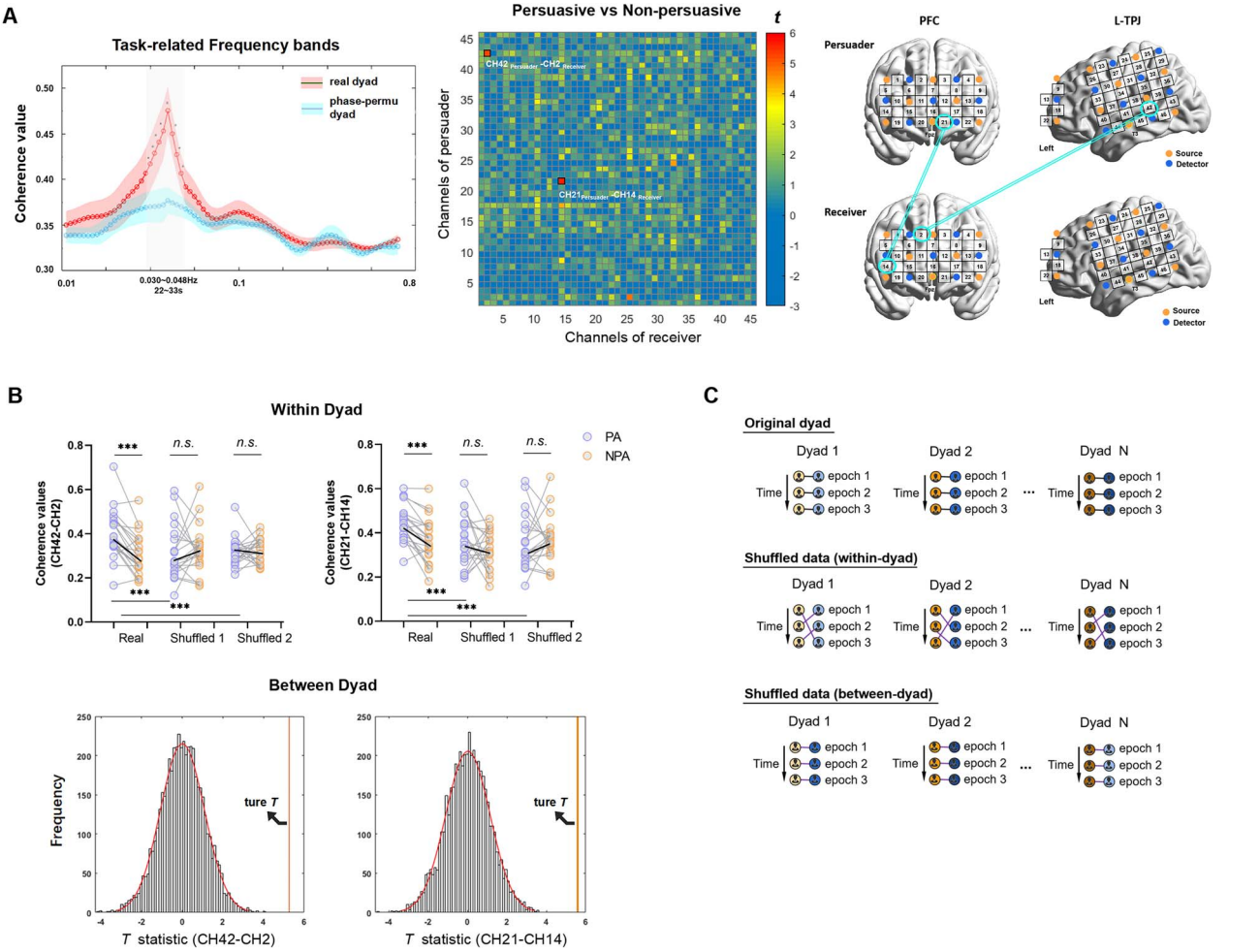

Fig. 2. Evaluation for persuasion on persuader-receiver neural coupling and validation tests. (A) Persuading-related neural coupling reached the highest level at the frequency range of 0.030–0.048 Hz (22–33 s) in comparison with phase permutation data sets. Within FOIs, neural coupling was calculated for all CHs, generating 46 × 46 matrices of *T*-values. Two significant CHs were identified, CH42-CH2 and CH21-CH14, the former is the persuader, and the latter is the receiver. (B) Two validation tests (upper: shuffled data within-dyad, lower: shuffled between-dyad) validate the observed persuading effect. The yellow lines indicate the positions of the true *T* values of the original dyads. (C) Validation statistics. Neural coupling measures are either calculated for the same dyads and yet randomizing items (shuffled data within-dyad. Shuffled1: Item01-Item02, Item02-Item03, Item03-Item01; Shuffled2: Item01-Item03, Item02-Item01; Item03-Item02, former is a persuader and later is the receiver) or between the dyads (shuffled data between-dyad).

triggered only two types of shuffled data sets (refer to Fig. 2C, shuffled data (within-dyad)). A parametric statistical significance testing approach tested the persuading effect on neural coupling in the identified significant CHs. Second, a validation test was applied to the shuffled-pair dyads. Particularly, HbO signals from all 42 female participants were re-shuffled randomly (e.g., HbO signals from persuader #1 were paired with those from receiver #2). Thus, 21 new dyads were created and the coherence values were recalculated. Accordingly, the persuading effect was re-analyzed to obtain the *T* value for shuffled-pair dyads. This procedure was conducted 2000 times to yield null distributions (*T* values) of significant CHs, significant levels ($P < 0.05$) were assessed by contrasting the *T* value from the original dyads with 2000 renditions of shuffled-pair dyads (Fig. 2C, shuffled data (between-dyad)).

Directional coupling

As our participants have clearly defined roles (where one person transmitted verbal arguments—persuader, and the other one received verbal arguments uttered by the other side—receiver), we are able to determine the preferred directionality of "information flow" between persuader and receiver in the experiment. Multivariate Granger Causality (MVGC) Toolbox was adopted to calculate the conditional G-causality in the time domain (Barnett and Seth 2014). After preprocessing (*2.4.2 fNIRS Data Preprocessing*), the HbO time series were normalized using z-transforms (i.e., converting persuading phase data into z-scores employing the mean and standard deviation of resting phase), which resulted in a relatively stable time series (Pan et al. 2021, Zhu et al., 2021). The data were further down-sampled to 1 Hz (Ono et al. 2021). Hereby, G-causality was conducted to estimate bidirection (i.e., from persuader (P) to the receiver (R) P → R, and from the receiver (R) → persuader (P) R → P) and magnitude of information flow between the two HbO time series on the CHs indicated a significant persuading effect, at PA and NPA, correspondingly.

Validation analysis of directional coupling

Intending to see whether G-causality indices found in the original data statistically differed from zero, the original data were phase-randomized as surrogate data sets (see section "*Determining the Frequency Ranges of Interest*" for a detailed method description). The

Table 1. Consequences of hierarchical regression: predicting persuasion outcomes at follow-up using subjective measures and neural coupling

Step	R^2	Adj.R^2	Res.*DF*	*F* values	Model sig.	R^2 change	*F* change	*F* change sig.	AIC
1 Subjective measurements	0.267	0.186	18	3.282	0.061				2.771
2 Neural coupling of PA	0.442	0.343	16	4.487	0.017	0.175	5.321	0.034*	2.484
3 Neural coupling of NPA	0.646	0.494	14	4.258	0.012	0.115	2.159	0.152	2.563

true G-causality indices derived from surrogate data sets serve as a "null distribution" for statistical inference. The empirical *P*-values derived from original data were determined from the distribution of 2000 permutated surrogate data sets, we defined *P*-value less than 0.05 as a significant difference was noted (Ono et al. 2021).

Linking persuasion outcomes with neuropsychological tests

Subsequently, to explore the possible relevance of the persuasion outcomes with neuropsychological measurements, a series of Pearson correlations (two-sided) was first performed to examine the potential contribution of subjective assessment (i.e., pre-scanning assessment and Post-scanning assessment) to persuasion outcomes (see Supplementary Tables S3 for the full description).

Then, Pearson's correlations (two-sided) were adopted to test the relationship between persuasion outcomes and neural coupling signatures (PA and NPA, separately). Moreover, to further evaluate the generalizability of brain–behavior relationship, we also implemented a data-driven, machine-learning method for predicting persuasion outcomes based on neural coupling using a leave-one-out cross-validation scheme, via least squares regression (LSR) algorithm. We standardized each category across participant dyads before performing the regression model. Out-of-sample performance was evaluated by calculating the Pearson *r* value between predicted and actual persuasion outcomes, significance of the *r* value was then tested against a null distribution of *r* values generated by permutation testing. We adopted shuffled data sets (generated in the "*Validation Analysis on Neural Coupling*" section) to repeat the entire data analytic procedure described above to generate a null distribution ($n = 2000$). *P*-values were determined by calculating the frequency with which the true model *r* value exceeded the *r* values in the null distribution.

Ultimately, to determining whether neural coupling measures can make a unique contribution, we performed a hierarchical linear regression model to infer the amount of additionally explained variance for the predictors-of-interest (The subjective assessments demonstrate a significant correlation with persuasion outcomes; neural coupling of PA and NPA from the significant CHs.) as reported in Table 1.

Dynamic neural coupling analyses in persuasive information conveying

What is lesser known is what exact processes that lead to people's attitudes or behavior change on the condition that they engaged in natural persuading. We, thereby, argue that neural coupling dynamic trajectory in persuasive information conveying may offer a new lens that means neural coupling might otherwise not be captured. Given that more than half of the items (58.7%) have been completed within 75 s, we removed the last ~15 s of each item time course to obtain data within a steady state. Given that temporal dynamic neural coupling may primarily reflect timely speech content perception and comprehension; nevertheless, persuading is a process that the receiver retention and accumulates information continually and thereby decides to accept or reject the arguments of the persuader. In light of this, both temporal and cumulative-temporal dynamic neural coupling were conducted. Specifically, for each dyad, the cumulative-temporal dynamic neural coupling at end time-point *n* was calculated as the average of neural coupling ranging from the first time-point to the *n*th time-point. A series of two-sided paired sample *t*-tests were conducted on temporal and cumulative-temporal dynamic neural coupling at each time point, resulting in a time-point of *P*-values. The resulting *P*-values were corrected by the FDR method (threshold: *P*-values < 0.05). We narrowed our focus to the CHs that exhibited significant persuading effects.

Eventually, to specify how dynamic neural coupling explains characteristics of persuasive behavior, we explore decoding video-recording data sets from the dynamic neural coupling. The time course of neural coupling was down-sampled to 1 Hz to obtain point-to-frame correspondence between the brain data sets and the verbal arguments. Furthermore, a machine learning approach (i.e., support vector machine (SVM) classification) was exploratory applied to identify whether the persuading effect can be decoded from the time course neural coupling datasets (in a similar manner to Barreto et al. 2021; Chen et al. 2022). A leave-one-out cross-validation (LOOCV) approach was employed to obtain the prediction accuracy. Permutation testing was used to generate a null distribution, against which the significance of prediction accuracy was evaluated. We took advantage of shuffled labels (PA vs. NPA) to recalculate the prediction accuracy 2000 times to yield a null distribution. *P*-value was determined by calculating the frequency with which the true values of prediction accuracy exceeded the null distribution (threshold: *P*-values < 0.05).

Results

PA prompt enhanced neural coupling than NPA

To confirm hypothesis 1, we submitted all CHs to paired samples *t*-tests (two-sided) within identified FOIs (0.030–0.048 Hz, 22–33 s). The results demonstrated stronger neural coupling in PA than NPA in the left superior temporal gyrus (STG) of the persuader and the superior frontal gyrus (SFG) of the receiver (CH42-CH2, $t_{20} = 5.262$, p(after FDR) = 0. 039, Cohen's $d = 2.35$), and superior frontal gyrus (SFG) of the persuader and inferior frontal gyrus (IFG) of the receiver (CH21-CH14, $t_{20} = 5.590$, p(after FDR) = 0. 038, Cohen's $d = 2.50$) (Fig. 2A, middle and right). No other significant results were discovered at any other CHs of this FOIs, nor at any other CHs of other frequency bands (FDR corrected *Ps* > 0.05). Moreover, to eliminate the possibility that the results were confounded by the differences in length of time, a statistical comparison of the

number of items counted by PA and NPA within each dyad was performed. No significant differences were found ($P > 0.1$, non-parametric Wilcoxon test due to data not normally distributed), eliminating the time length effect on the results reported here.

Validating the main neural coupling findings

Two validation approaches were conducted. First, the approach on shuffled data within the dyad did not show any significant persuading effects in the two shuffled data sets (Fig. 2B upper, $-0.43 \leq ts \leq 1.38$, $Ps > 0.05$). Moreover, neural coupling in the PA from the original dyads was significantly higher than from the shuffled data sets ($ts > 3.97$, $Ps < 0.05$, Cohen's $d \geq 1.77$) but no significant differences were found between the NPA and the shuffled data-sets ($-1.98 \leq ts \leq 1.68$, $Ps > 0.05$), suggesting that the identified neural coupling in the current study was specific to the timely PA. Second, the approach on shuffled data between dyads indicated that the null distributions did not demonstrate any significant persuading effect ($Ps > 0.05$ after FDR correction, null distributions shown in Fig. 2B, lower). Furthermore, in comparison with the distribution generated by shuffled data, the T values of the real dyads significantly exceeded that of the shuffled-data null distributions, with significant empirical P-values ($Ps < 0.001$. Fig. 2B, lower). Collectively, our findings indicated that PA effectively induce robust neural coupling and this coupling-based persuading effect was specific to actual interaction in the real persuader-receiver dyads.

Directional coupling results

From two significant CHs, the G-causality indices (i.e., P → R, R → P) were calculated with original and surrogate data sets, in which the latter one was adopted to validate the statistical significance of causal strength from original data. As indicated in Fig. 3A, in the CH42-CH2, a significantly biased directionality with G-causality indices from P → R (M ± SD, 0.046 ± 0.036) larger than that from R → P (M ± SD, 0.029 ± 0.013) was found on the PA ($t_{20} = 2.42$, corrected $P = 0.047$, Cohen's $d = 1.08$), and yet exhibited no significant difference in terms of the NPA's directionality (P → R vs. R → P: 0.035 ± 0.029 vs. 0.036 ± 0.033, $P > 0.05$). Nonetheless, in the CH21-CH14, there were no significant differences in terms of the G-causality indices both on PA and NPA (PA: P → R vs. R → P, 0.056 ± 0.012 vs. 0.043 ± 0.013; NPA: P → R vs. R → P, 0.036 ± 0.005 vs. 0.033 ± 0.004, $Ps > 0.5$, Fig. 3B).

In the following, phase-randomized test to respectively examine whether the values of R → P and P → R G-causality were considerably greater than the "null distribution." On the PA, the original HbO signals in the CH42-CH2 showed valid bidirectional G-causality indices, as the real indices of R → P and P → R were both substantially larger than surrogate data-sets ($Ps < 0.01$) (Fig. 3C PA), but not in P → R and R → P in the NPA ($Ps > 0.05$, Fig. 3C, NPA condition). It appears that significant and comparable bidirectional information flow existed between the persuader and receiver at CH42-CH2 during the transmission of PA. On the contrary, only unidirectional coupling from persuader to receiver (P → R) was found on the PA at CH21-CH14 (Fig. 3D, PA condition). Additionally, similar to CH42-CH2, no significant valid G-causality indices were found on the CH21-CH14 NPA, both P → R and R → P ($Ps > 0.05$, Fig. 3D, NPA condition).

Relationship between subjective measurements, neural coupling, and the persuasion outcomes

Prior to investigating neural coupling differences between the PA and NPA, we also examined whether there were distinctions between PA and NPA in how the receiver rating the arguments. On the basis of the receivers' evaluation, the convincement confirmed the distinction into PA (M ± SD, 6.55 ± 1.31) as in comparison with NPA (M ± SD, 4.98 ± 1.89), $t_{20} = 4.21$, $P < 0.001$, Cohen's $d = 1.88$, paired samples t-test, two-sided; whereas no effect of evaluation on concreteness (PA: M ± SD, 7.42 ± 1.00; NPA: M ± SD, 6.98 ± 1.91) or amusement (PA: M ± SD, 6.29 ± 1.50; NPA: M ± SD, 6.13 ± 1.84), $0.32 \leq ts \leq 1.43$, $ps > 0.1$, paired samples t-test, two-sided, Fig. 4A-C. We thus argue that the effectiveness of persuading was significantly influenced by the receiver's perceived convincement of the arguments, yet not the concreteness or amusements.

Pearson correlation analyses were employed to directly test the relationship between receivers' evaluation and persuasion outcomes. The sum of three items' ratings represented receivers' evaluations. Predictably, the results revealed a strong positive correlation between the persuasion outcomes and convincement rating ($r = 0.47$, $P = 0.032$, Fig. 4D), and yet not to the concreteness or amusement rating (all $rs < 0.27$, $ps > 0.1$). Except for that, a positive correlation was found between receiver-persuaded perception and persuasion outcomes ($r = 0.47$, $P = 0.033$, Fig. 4E). Moreover, repeated Pearson correlation analyses were conducted on the persuasion outcomes as well as other self-report measurements (such as personality traits, STPS, confidence rating, etc.). Yet none of these measurements were correlated with persuasion outcomes, ruling out alternative psychological explanations for persuasion outcomes we found (Further breakdown of findings can be found in Supplementary Table S3 for detailed descriptions.)

Subsequently, under PA and NPA, correlation analyses were conducted to examine the potential relationship between persuasion outcomes and neural coupling from significant CHs. correspondingly. Results confirmed there was a positive correlation between persuasion outcomes and the neural coupling in the PA ($r = 0.54$, $P = 0.012$) but not in the NPA ($r = -0.12$, $P > 0.05$) at CH42-CH2. Moreover, at CH21-CH14, no significant correlations were found in PA and NPA conditions both (PA: $r = 0.33$; NPA: $r = 0.20$, $Ps > 0.05$).

Furthermore, considering that the current finding has limited statistical power due to the small sample size, additional prediction modes were utilized to assess the generalizability of the brain–behavior relationships. Since the positive correlation between persuasion outcomes and neural coupling in two CHs in the PA ($rs > 0.33$), we speculated neural coupling of PA, rather than NPA, could effectively predict the persuasion outcomes. The prediction model was developed to use the neural coupling in the PA or NPA as inputs to generate predictions of the outcomes of persuasion. Results demonstrated that the actual persuasion outcome was significantly correlated with what was predicted by the model of PA, with predictive power significantly greater than the majority of the 2000 permuted r-values ($r_{20} = 0.41$, $P = 0.035$, Fig. 4F). Nonetheless, neural coupling in the NPA did not predict persuasion outcomes ($r_{20} = 0.26$, $P > 0.05$). Moreover, we replicated this finding by re-adding the removed dyads (PA: $r_{23} = 0.46$, $P = 0.027$; NPA: $r_{22} = 0.24$, $P > 0.05$).

Eventually, to determine whether neural coupling measures (particularly in PA) could make a unique contribution, a hierarchical linear regression analysis was conducted with persuasion outcomes as the dependent variable. We began by entering subjective measurements (convincement rating, receiver persuaded perception). Subsequently, neural coupling of PA in the next step, neural coupling of NPA in the last step. As reported in Table 1, entering neural coupling of the PA explained an additional 17.5%

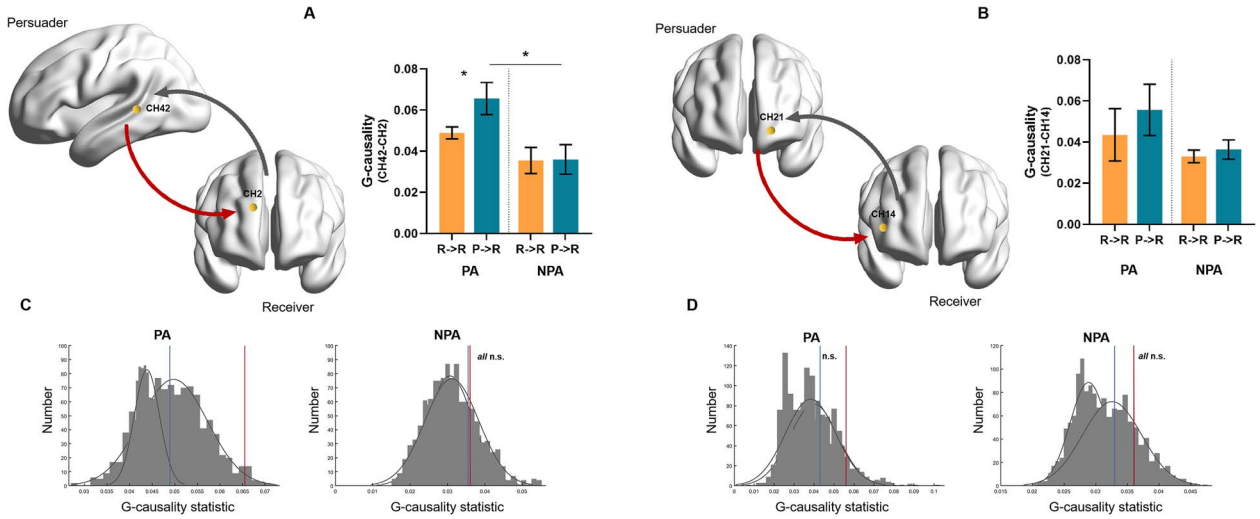

Fig. 3. Results of G-causality statistic P → R and R → P for CH42-CH2 (*A* and *C*). Note that G-causality indices of P → R and R → P were both substantially above zero for the PA and higher G-causality indices of P → R than R → P. (*B* and *D*) G-causality statistic for CH21-CH14. G-causality P → R was significantly greater than zero on the PA. P → R: From persuader to the receiver; R → P: From receiver to persuader. The red line indicates P → R; the blue line indicates real R → P; *n.s.* indicate the true G-causality indices do not significantly exceed the null distribution. *$P < 0.05$. PA: persuasive arguments; NPA: non-persuasive arguments.

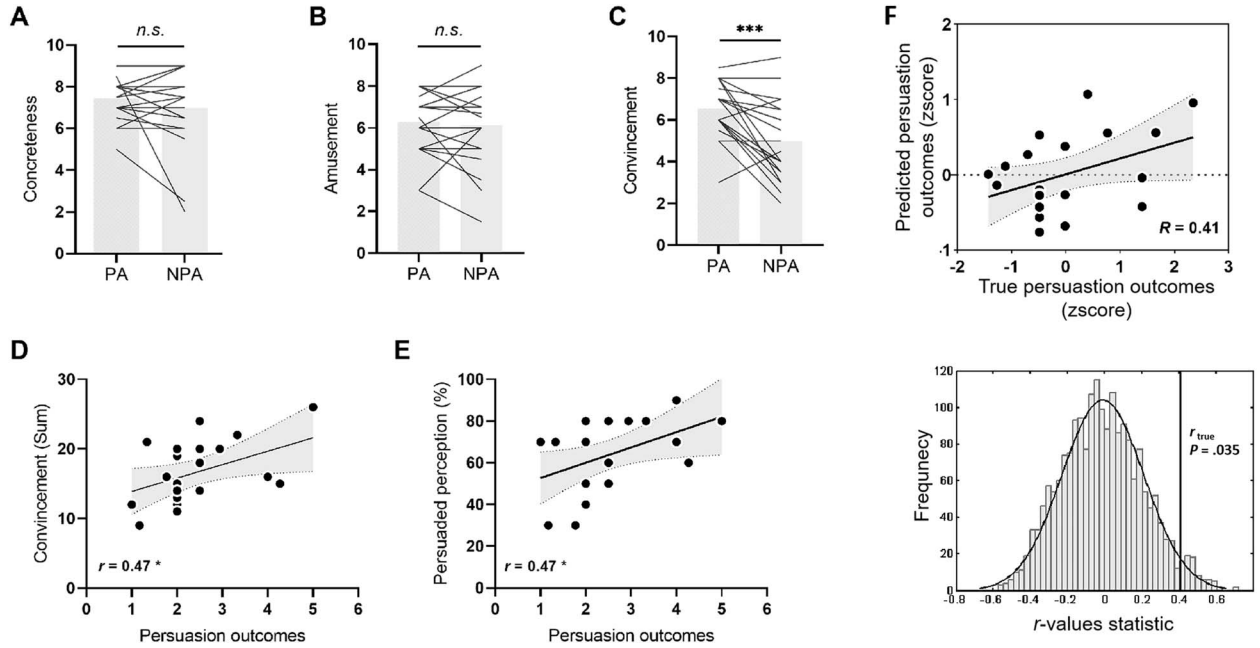

Fig. 4. The link between persuasion outcomes and subjective assessments, neural coupling. (*A*-*C*) Convincement rating showed a significant difference that higher ratings in PA than in NPA. There were no significant differences in the ratings for concreteness and amusement between PA and NPA. (*D*) A positive correlation between convincement rating and persuasion outcomes. (*E*) A positive correlation between receiver persuaded perception and persuasion outcomes. (*F*) The neural coupling in PA accurately predicted the outcomes of persuasion. The prediction performance was evaluated through the correlation between the actual and predicted persuasion outcomes. The significance of this relationship was determined through permutation testing. *$P < 0.05$, **$P < 0.01$, ***$P < 0.001$. PA: Persuasive arguments; NPA: non-persuasive arguments.

of the variance, resulting in a better model fit ($F_{change} = 5.321$, $P = 0.034$). Nonetheless, adding neural coupling of the NPA did not explain additional variance ($F_{change} = 2.159$ $P > 0.05$). A supplementary analysis further confirmed the specific contribution of the neural coupling of PA to the persuasion outcomes as we entered the neural coupling of PA, NPA, and subjective measurements, in order. Results demonstrated that additional neural coupling of NAP or subjective measurements did not account for variance in persuasion outcomes ($Fs_{change} < 2.817$, $ps > 0.05$, see Supplementary Table S4).

Dynamics of neural coupling during arguments conveying and corresponding persuading behavior decoding

Based on the time point of corrected *P*-values, the primary results as described: (i) In CH42-CH2, the temporal dynamics analyses exhibited multiple time windows of significant differences between PA and NPA (i.e., from 16 to 34 s, from 44 to 57 s. see Fig. 5A, gray panels); (ii) the distinction in CH21-CH14 temporal dynamic emerged at a relatively late time window by started at 53 s and this differentiates persisted into the end of informing

(see Fig. 5C, gray panels); (iii) the cumulative-temporal dynamic analyses confirmed that shortly after the beginning of informing, neural couplings could stably distinguish between PA and NPA (22 s at CH42-CH2. About, 28 s at CH21-CH14, FDR correction. Figure 5B and D), and these effects were robust enough to persist into the end of informing.

Given that cumulative-temporal dynamic neural coupling might mark where persuading occur, we further combine these watershed time points with video-recording data sets to interpret the psychological significance of these findings. It is worth noting that the earliest significant time points (22 s, 28 s) were nearly in sync with the frequency bands in the present research (frequency bands: 22–33 s) that is associated with the periods of persuading, which possibly suggest that the receiver have been decided to accept or reject the arguments after the first case of arguments elucidated. To substantiate this conjecture, two additional coders (naïve with regard to the purpose of the study) were recruited to independently and manually code persuading behaviors in subsets of the dual-fNIRS scanning phase for the video (two-thirds of the data sets each). Coding was performed on a 1-s time scale. Here, we predominantly focus on the persuaders' vocal statements and the arguments of each item were further segmented into several cases (an example see Fig. 5E and F). Each coder trained in the quantization of the number of cases as well as the began and ended time(s) corresponding with each case, within each item. For all coding activities, inter-coder reliability was calculated by the intra-class correlation (ICC, Werts et al. 1974). The inter-coder reliability was satisfactory (Cronbach's alpha = 0.93). Eventually, data sets were obtained by averaging and rounding across the two coders. Based on coding procedures, persuaders spend 9–39 s (an average of approximately 21 s) for the first case of each item, similar to the earliest time at neural coupling can distinguish whether persuaded or not (The jointly video-recording data sets for all participant dyads seen in the Supplementary Table S6).

To further verify the statistical significance of the above finding, the SVM classification algorithm was exploratorily employed to identify the EPOCH for discriminating persuading effect at the individual level. Specifically, based on the findings above, the arguments of each item were divided into two EPOCHs (EPOCH1: the averaged coherence values of the first case; EPOCH2: the averaged coherence values of the rest cases). Accordingly, the classifier predicted the persuading (PA vs NPA) utilizing each EPOCH (EPOCH1, EPOCH2) neural coupling from identified significant CHs as classification features. Except for that, we likewise conducted analyses to examine the classification effect on the EPOCH (EPOCH1 vs EPOCH2). Results further demonstrated that the classifier of neural coupling reliably and distinguished PA and NPA at EPOCH2 in significant CHs in both temporal and cumulative-temporal dynamic neural coupling (Prediction Accuracy range from 0.66 to 0.70), but not at EPOCH1 (prediction accuracy < 0.59, $Ps > 0.05$). (More details can be found in the Supplementary "SVM classification approach identify EPOCH for discriminated persuading effect").

Discussion

Using a naturalistic dyadic persuasion paradigm (NDP) and a dual-fNIRS technique to capture shared neural representations between persuader and receiver, we examined the neurobiological basis of human persuasion. Broadly, the current findings provided evidence in support of our primary hypotheses that PA increase neural coupling more than NPA. Critically, the neural coupling of PA successfully predicts persuasion outcomes. Eventually, dynamics of neural coupling incorporating video-recording data sets and machine learning approach investigated that after the first case of argument, the neural coupling would sensitively discriminate persuaded or not, this finding might signal the time-point by where persuasion takes hold. The implications of these findings are discussed in the following section.

How might neural coupling during naturalistic persuading mark arguments persuasiveness?

In this study, higher neural couplings between persuader and receiver in the persuasiveness of the argument compared to the arguments that were not persuasive. Some control analyses further excluded the potential confound of this effect (i.e., length of time, validation analyses). Moreover, G-causality findings have deepened our comprehension of information "flow" at the neurophysiological level of persuading. And our finding was consistent with a dual-stream model for language processing (Hickok and Poeppel 2007) that directional coupling phase-randomized test revealed bidirectional information flows of the neuronal signal during the persuasion identification stage at PA condition in the CH42-CH2, suggesting rather than simply simple one-way information transmitting from persuader to receiver, the receiver would also positively comprehend and predict the incoming information during persuading (Yan et al. 2012; Lee and Shin 2021). Conversely, on the condition that arguments were unrecognized by the receiver (NPA condition), the information flows in the neuronal signal were weakened and largely elusive. Higher information flow from persuader to a receiver in PA than in NPA also suggests that compared to NPA, PA are more valid and compelling to receivers. Therefore, the present findings provided supportive evidence for the perspective that neural coupling is a potential interpersonal neural pathway involved in translating messages into effects on individuals, as well as quantified inter-individual information flows directionality during live persuading at the neurophysiological level.

Moreover, relevant brain areas are close to the persuader's subregions of the prefrontal and left temporo-parietal, approximately located at the superior frontal gyrus (CH21, SFG) and left superior temporal gyrus (CH42, STG); and the receiver's subregions of the prefrontal, approximately located at superior frontal gyrus (CH2, SFG) and inferior frontal gyrus (CH14, IFG). IFG was essential for decoding intentions and objectives during social cognition and interaction (Hamilton and Grafton 2008; Keller et al. 2014). In a study on social influence, IFG was reported during social conformity (Charpentier et al. 2014), and increased activity in the IFG during preference shifts toward others' preferences. (Izuma and Adolphs 2013). Furthermore, IFG-related neural coupling has been found involving promote social interactions by predicting each other actions and intentions, including verbal interaction (Jiang et al. 2012), interactive learning (Pan et al. 2020, 2021), unstructured game-playing (Li et al. 2021). In accordance with these views, neural coupling at IFG may facilitate receiver incorporation of arguments, by internalizing the persuader's knowledge, belief, and intention.

STG and SFG are closely associated with the mentalizing system (Baker et al. 2016), a set of brain regions involved in thinking and reasoning mental states of others (Carter and Huettel 2013; Lieberman et al. 2019). Previous research has demonstrated that the mentalizing system involved in persuasion relevant processes in persuader, such as considerations of the information's meaning to receivers and the potential for positive social interactions with others (Baek et al. 2017), predicting the likelihood of a message

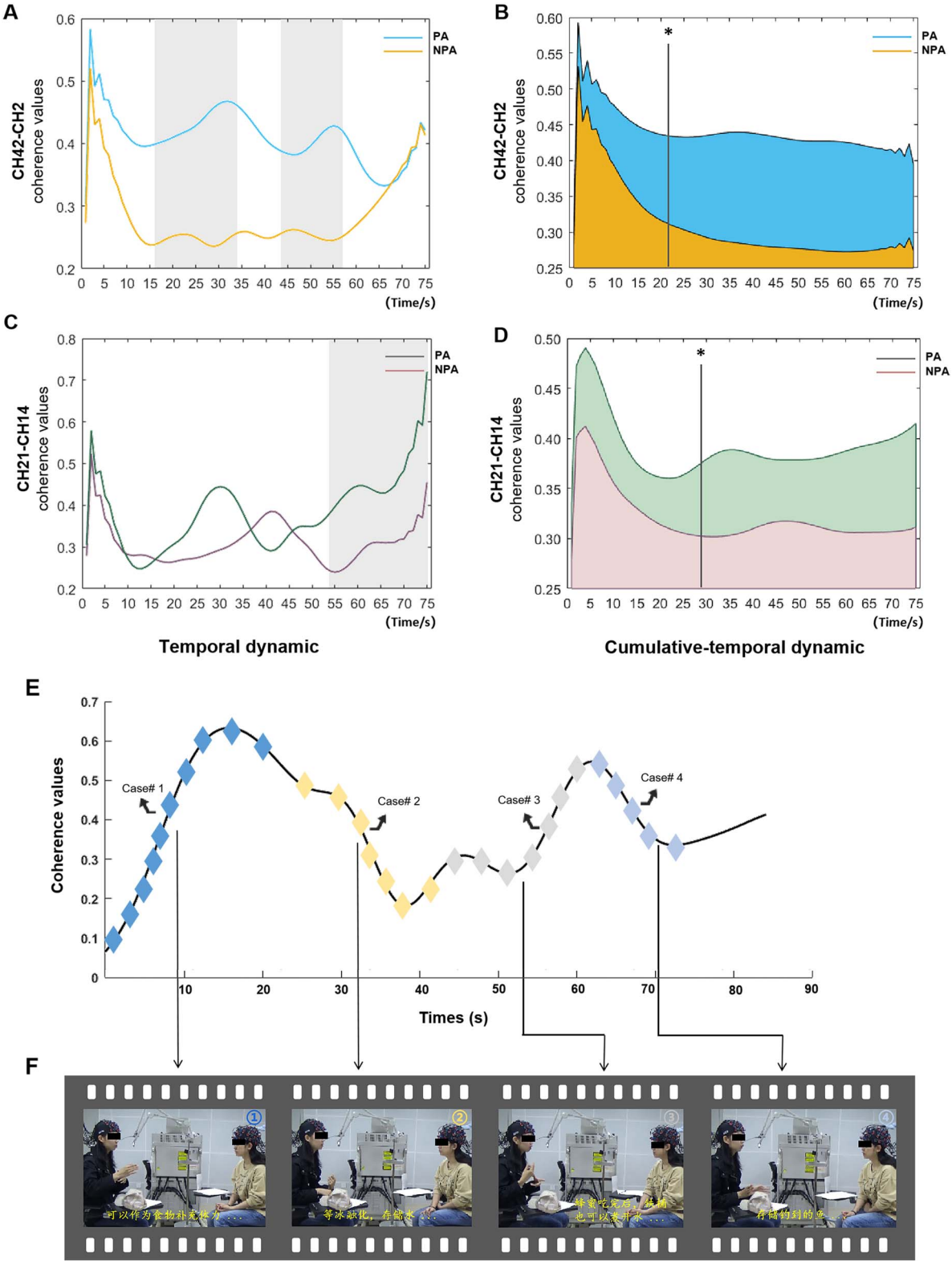

Fig. 5. Dynamics neural coupling during persuasive information conveying and persuading behavior decoding. The temporal dynamic neural coupling in PA and NPA for the significant CHs (*A* and *C*). Gray panels indicate distinction reached significance in temporal dynamic neural coupling between PA and NPA at *P*-values < 0.05 with FDR correction. The cumulative-temporal dynamic neural coupling in PA and NPA for the significant CHs (*B* and *D*). The vertical lines with asterisks indicate the distinction reached significance in cumulative-temporal dynamic neural coupling between PA and NPA at *P*-values < 0.05 with FDR correction. (*E*) Example of the temporal evolution of neural coupling during a persuasion task. Distribution of time for cases across the entire time course of coherence values by color-coded rhombus. (*F*) Example video frames coding persuading behaviors. Four cases and corresponding predominant contents persuader to elucidate why she thought *Can of honey* more important. The numbers 1, 2, 3, and 4 in color-coded displayed the principal contents that correspond to the time course of neural coupling in *E*.

reaching its intended recipient (Scholz et al. 2017), and how successful in convincing them (Dietvorst et al. 2009; Falk et al. 2013). Moreover, mentalizing system (i.e., SFG) was found reflect differences of persuasiveness in the message (i.e., high- and low-tailored messages), rather than persuasiveness of message per se (Kato et al. 2009). Our finding also aligns with this finding, as significant CHs were based on the arguments persuasiveness or not (i.e., PA vs NPA).

Taken together, our study further supports the idea that neural coupling in these areas reflects a potential social neural mechanism for the successful information propagation between persuaders and receivers and persuasion.

How might neural coupling during naturalistic persuading predict persuasion outcome?

Early studies in the "brain-as-predictor" tradition within the field of persuasion have frequently focused on single-brain activation (such as Falk et al. 2010, 2011). Our current findings complement and extend this framework by demonstrating that neural coupling is a key predictor of the persuasion outcomes (i.e., receiver's compliance). Crucially, we found neural coupling in the PA, rather than in the NPA, would successfully predict persuasion outcomes. In our study, persuasion outcomes were quantified by weighing the ranking order of changed items, the items that were not selected were marked as "0." Thereby, if only PA (i.e., the changed items) have an effect on persuasion outcomes, neural coupling in PA, as opposed to NPA (i.e., the no changed items), could accurately predict the degree of persuasion outcomes. Likewise, we contend persuasion outcomes in our study were mainly contributed by PA, but not by PNA. Accordingly, current results in prediction mode and hierarchical linear regression confirmed this inference. More importantly, consistent with prior research (Imhof et al. 2020), our findings demonstrated that neural coupling appears to be a better predict persuasion outcomes than self-reported identification, as a hierarchical linear regression approach using neural coupling in PA condition explained an additional 17.5% extra variance over self-report measures.

Despite slightly less prediction, it should be noted that self-report assessments are also meant to provide some unique views. Firstly, the persuasiveness of arguments was generally dependent on perceived convincing, whereas perceived concreting or amusing was inadequate to determine the persuasiveness of arguments. Similarly, the persuasion outcomes were high relevance with greater perceived convincing of the arguments, and yet not perceived concreting or amusing. Secondly, the receiver persuaded perception was positively associated with persuasion outcomes, nonetheless, instead, the persuader's persuade perception did not show significant correlations with persuasion outcomes (see Supplementary Table S3). One interpretation is that persuader did not gain feedback from the receiver during the experiment, though this setting excluded potential confounds arising from complex interpersonal interaction, the persuader assess persuasion outcomes barely on the basis of their own subjective evaluation, and some nonverbal signals from the receiver (i.e., eye contact, head nods) which may obscuring the perception of persuasion effects (i.e., nodding may reflect continuous attention but not the approve of her views) (Chen et al. 2013; Baek and Falk 2018). The receiver's feedback could promote the persuader's more accurate assessment of the argument-outcome link and hence promote the effectiveness of persuading; this proposition seems significant for future research.

How might spatial and temporal properties of neural coupling elucidate persuading processing?

Two distinct spatial patterns of neural coupling (STG-SFG, SFG-IFG) might be expected to mark distinct stages of persuading. Here we confirmed this speculation by incorporating past theories and our current results.

From Aquino et al. (2020), successful persuasion predominantly involves two basic stages: information identification and internalization. During the information identifying stage, the persuader starts to communicate ideas and intentions to the receiver, receiver implicitly thinks about the content of these messages, evaluating and reflecting on the value for themselves; whereas, during the internalization stage, the receiver generates their attitude ("I think you are right/wrong," "I accept/reject this idea"). When incoming information changed receivers' ideas, they are more likely to update their initial views or behaviors and internalize new ideas, to be consistent with the persuader (Aquino et al. 2020). Consequently, the neural coupling of STG-SFG and SFG-IFG in the present study may correspond to the identification and internalization stages, or vice versa.

Furthermore, in temporal dynamics results, neural coupling at STG-SFG exhibited an early significant persuasive effect during argument transmission (range from 16 to 34 s, 44 to 57 s), SFG-IFG neural coupling indicated a significant persuading effect at a relatively later stage (after 53 s). Consequently, the neural coupling in STG-SFG might mark the identification stage and SFG-IFG might indicate the internalization phase of persuasion. Taken one step further, the internalization stage mostly reflects the degree of the receiver to internalized and updating views conveyed by the persuader, and thus, in G-causality, only unidirectional information flows of P → R in the PA in the STG-SFG, rather than flows of R → P. Acknowledging that the aforementioned hypothesis is still speculative and is awaiting further research for verification.

How might neural coupling during naturalistic persuading identify when persuading take hold?

Ultimately, dynamic neural coupling measures provide evidence at the moment that persuading takes hold. Some past research has confirmed the validity of this approach (Jiang et al. 2015; Liu et al. 2019). For instance, Jiang et al. (2015) found leader emergence can be predicted by the neural coupling shortly after the start of the leaderless group discussion task (about half a minute into the interaction). In the current study, we found approximately 22 s after arguments informing, the neural coupling could successfully infer whether people be either persuaded or not. To go a step further with it, we interpreted the psychological significance of the finding by combination video-recording data sets, the initial instance (i.e., the first case of the arguments) with the target items may be valuable as a first step in encouraging the receiver's change. Our investigation has provided evidence in support of this primary conclusion as (i) overlap between the time-points of the cumulative-temporal dynamic neural coupling for distinguishing PA and NPA and the initial instance of argumentation that was captured on video-recording; (ii) statistical evidence (i.e., SVM classification) for after the first case of arguments elucidated, neural coupling of EPOCH2 could reliably and manage to infer PA and NPA.

Notably, whether our finding indicates the rest cases of arguments as a form of redundancy? One relevant study by Bleakley et al. (2020) found focus on one or a few preferred courses of action may make it more likely that one will end up with more determined goals. Nonetheless, in the present study, we only

found a weak effect of EPOCH in NPA (the decrease of neural coupling in the EPOCH2 compared to EPOCH1), but not in PA. Consequently, one possible explanation is that the receivers are motivated to continuously attend and focus on the PA, and thus, all cases, as a receiver, perceive as salient. Whereas, if the first case is not persuasive or even produces a counter-attitudinal (i.e., NPA), to avoid dissonance, it could lead to receivers adopting a processing-reduced and prevention-focused approach to subsequent information evaluation. Remarkably, the neural coupling could sensitively track and discriminate this psychological processing. In conclusion, these novel findings contribute significantly to research on attitude formation and persuasion as well as social cognitive neuroscience in general.

Limitations and future directions

We merely recruited female–female dyads due to our initial data gathering males being largely immune to persuasion. Relies on psychological reactance theory (PRT, Brehm 1966; Brehm and Brehm 2013), people are wary of being persuaded if they know someone is attempting to do so, it frequently backfires (Campbell and Kirmani 2000; Kirmani and Zhu 2007). Here we find this effect is particularly noticeable in male participants, even though we used words such as "provide some ideas to you for reference only," and "decision is yours" to replace "persuasion you" in the instruction. Nonetheless, it is with regret that this variable did not measure in the present study, and yet we considered at least in a current research context, gender-specificity may have unpredictable effects on persuasion. Obviously, this does not imply that gender-effect is irrelevant, we encourage researchers to avoid treating this variable as direct measures of persuasiveness and instead consider when and why they are associated with persuasion, persistent over time, and influence for thought and behavior.

Additionally, the NDP paradigm provides a template to access neural coupling that is responsive to naturalistic persuading, nonetheless, we employed an ecologically valid yet experimentally controlled setting with, a lack of bidirectional verbal interaction between persuader and receiver. Indeed, the persuader could be able to timely adjust their persuasion strategies and interventions based on the receiver's response to anticipate and shape anticipated receiver responses, thereby promoting persuasion. Thus, the experimental situations allowing the persuader and receiver to adopt an active and more realistic role in persuading, and simultaneously recording participants' hand and body movements, eye movements, facial expressions, and physiological changes between interlocutors, is urgently required. Subsequently, a more diverse sample including more variation in socioeconomic status and ethnicity, and more types of social contexts including doctor-patient communication, and seller–buyer would increase generalizability. Most substantially, we presume the putative underlying mechanism for neural coupling will be fruitful to track the persuasion interactive process and involve differentiable patterns of interactive models and persuasion strategies.

Finally, it was undeniable that fNIRS equipment partly limited current results for limited cortex region of interest, rather than global scalp parameters, and it cannot collect data from deep brain structures (including the precuneus, ventromedial prefrontal cortex, anterior cingulate cortex, etc.). Notwithstanding, this may change as fNIRS engineering advances and trustworthy computational methods to infer deep brain activity by measuring cortical activity are developed to compensate for the limitations of techniques centered on the cortex (Reiss et al. 2015).

Conclusion

In conclusion, this study examined the central hypothesis that persuader-receiver neural coupling underlies persuasion, by demonstrating that PA induce larger neural coupling than NPA and be a better predictor of persuasion outcome relative to traditional self-report measures. Moreover, dynamic neural coupling incorporating video-recording track dynamic persuading throughout ongoing arguments messaging and thus as an essential implicit measure to predict the condition that persuading take hold. This dyadic neuroimaging strategy has the potential to advance our understanding of the dynamic nature of the neurocognitive processes underlying persuasion.

Acknowledgments

We would like to thank Jieqiong Liu, Ruqian Zhang, and Mei Chen for their valuable comments on earlier drafts. Yiyang Xu, and Kaijia Yang for assistance in video coding. Bo Yang for revision the manuscript. This research was funded by the National Natural Science Foundation of China (32071082 and 71942001), Key Specialist Projects of Shanghai Municipal Commission of Health and Family Planning (ZK2015B01), and the Programs Foundation of Shanghai Municipal Commission of Health and Family Planning (201540114).

Supplementary material

Supplementary material is available at *Cerebral Cortex* online.

Funding

This research was funded by the National Natural Science Foundation of China (32071082 and 71942001), Key Specialist Projects of Shanghai Municipal Commission of Health and Family Planning (ZK2015B01), and the Programs Foundation of Shanghai Municipal Commission of Health and Family Planning (201540114).

Conflict of interest statement: The author(s) declared that there were no conflicts of interest with respect to the authorship or the publication of this article.

Data availability

The videos containing information that could compromise the privacy of research participants would not be publicly available.

Author contributions

Yangzhuo Li: formulated the research question, contributed to the study design, programmed and coordinated data collection, contributed to the analytic ideas, analyzed the data, visualization, wrote the paper. **Xiaoxiao Luo**: contributed to the study design, contributed to the analytic ideas, contributed to writing—review and editing the paper. **Keying Wang**: contributed to the analytic ideas, conducted video coding of the data. **Xianchun Li**: contributed to conceptualization, funding acquisition, supervision, writing—review & editing.

References

Anders S, Verrel J, Haynes JD, Ethofer T. Pseudo-hyperscanning shows common neural activity during face-to-face communication of affect to be associated with shared affective feelings but not with mere emotion recognition. *Cortex*. 2020:131:210–220.

Aquino A, Alparone FR, Pagliaro S, Haddock G, Maio GR, Perrucci MG, Ebisch SJ. Sense or sensibility? The neuro-functional basis of the structural matching effect in persuasion. *Cogn Affect Behav Neurosci*. 2020:20:536–550.

Ayrolles A, Brun F, Chen P, Djalovski A, Beauxis Y, Delorme R, Bourgeron T, Dikker S, Dumas G. HyPyP: a Hyperscanning python pipeline for inter-brain connectivity analysis. *Soc Cogn Affect Neurosci*. 2021:16:72–83.

Baek EC, Falk EB. Persuasion and influence: what makes a successful persuader? *Curr Opin Psychol*. 2018:24:53–57.

Baek EC, Scholz C, O'Donnell MB, Falk EB. The value of sharing information: a neural account of information transmission. *Psychol Sci*. 2017:28:851–861.

Baker JM, Liu N, Cui X, Vrticka P, Saggar M, Hosseini SH, Reiss AL. Sex differences in neural and behavioral signatures of cooperation revealed by fNIRS hyperscanning. *Sci Rep*. 2016:6(1):26492.

Barnett L, Seth AK. The MVGC multivariate granger causality toolbox: a new approach to granger-causal inference. *J Neurosci Methods*. 2014:223:50–68.

Barreto C, Bruneri GDA, Brockington G, Ayaz H, Sato JR. A new statistical approach for fNIRS Hyperscanning to predict brain activity of Preschoolers' using Teacher's. *Front Hum Neurosci*. 2021:15:622146.

Benjamini Y, Hochberg Y. Controlling the false discovery rate: a practical and powerful approach to multiple testing. *J R Stat Soc Ser B*. 1995:57(1):289–300.

Bleakley A, Jordan AB, Strasser AA, Lazovich D, Glanz K. Testing general versus specific behavioral focus in messaging for the promotion of sun protection behaviors. *Ann Behav Med*. 2020:54:108–118.

Boas DA, Elwell CE, Ferrari M, Taga G. Twenty years of functional near-infrared spectroscopy: introduction for the special issue. *NeuroImage*. 2014:85:1–5.

Brehm JW. *A theory of psychological reactance*. New York: Academic Press; 1966.

Brehm SS, Brehm JW. *Psychological reactance: a theory of freedom and control*. New York: Academic Press; 2013.

Burns SM, Barnes LN, Katzman PL, Ames DL, Falk EB, Lieberman MD. A functional near infrared spectroscopy (fNIRS) replication of the sunscreen persuasion paradigm. *Soc Cogn Affect Neurosci*. 2018:13(6):628–636.

Burns SM, Barnes LN, McCulloh IA, Dagher MM, Falk EB, Storey JD, Lieberman MD. Making social neuroscience less WEIRD: using fNIRS to measure neural signatures of persuasive influence in a Middle East participant sample. *J Pers Soc Psychol*. 2019:116(3):e1–e11.

Cacioppo JT, Petty RE, Feng Kao C. The efficient assessment of need for cognition. *J Pers Assess*. 1984:48(3):306–307.

Cacioppo JT, Cacioppo S, Petty RE. The neuroscience of persuasion: a review with an emphasis on issues and opportunities. *Soc Neurosci*. 2018:13(2):129–172.

Campbell MC, Kirmani A. Consumers' use of persuasion knowledge: the effects of accessibility and cognitive capacity on perceptions of an influence agent. *J Consum Res*. 2000:27(1):69–83.

Carter RM, Huettel SA. A nexus model of the temporal-parietal junction. *Trends Cogn Sci*. 2013:17(7):328–336.

Cascio CN, Scholz C, Falk EB. Social influence and the brain: persuasion, susceptibility to influence and retransmission. *Curr Opin Behav Sci*. 2015:3:51–57.

Chang C, Glover GH. Time–frequency dynamics of resting-state brain connectivity measured with fMRI. *NeuroImage*. 2010:50(1):81–98.

Charpentier CJ, Moutsiana C, Garrett N, Sharot T. The brain's temporal dynamics from a collective decision to individual action. *J Neurosci*. 2014:34:5816–5823.

Chen FS, Minson JA, Schöne M, Heinrichs M. In the eye of the beholder: eye contact increases resistance to persuasion. *Psychol Sci*. 2013:24(11):2254–2261.

Chen D, Zhang R, Liu J, Wang P, Bei L, Liu CC, Li X. Gamma-band neural coupling during conceptual alignment. *Hum Brain Mapp*. 2022:43:2992–3006.

Cheng X, Zhu Y, Hu Y, Zhou X, Pan Y, Hu Y. Integration of social status and trust through interpersonal brain synchronization. *NeuroImage*. 2022:246:118777.

Cooper N, Tompson S, O'Donnell MB, Emily BF. Brain activity in self- and value-related regions in response to online antismoking messages predicts behavior change. *J Media Psychol*. 2015:27(3):93–109.

Cooper N, Bassett DS, Falk EB. Coherent activity between brain regions that code for value is linked to the malleability of human behavior. *Sci Rep*. 2017:7:1–10.

Cope M, Delpy DT. System for long-term measurement of cerebral blood and tissue oxygenation on newborn infants by near infrared transillumination. *Med Biol Eng Comput*. 1988:26:289–294.

Dai B, Chen C, Long Y, Zheng L, Zhao H, Bai X, Liu W, Zhang Y, Liu L, Guo T, et al. Neural mechanisms for selectively tuning in to the target speaker in a naturalistic noisy situation. *Nat Commun*. 2018:9:1–12.

Davis MH. Measuring individual differences in empathy: evidence for a multidimensional approach. *J Pers Soc Psychol*. 1983:44(1):113–126.

Dietvorst RC, Verbeke WJM, Bagozzi RP, Yoon C, Smits M, van der Lugt A. A sales force–specific theory-of-mind scale: tests of its validity by classical methods and functional magnetic resonance imaging. *J Mark Res*. 2009:46(5):653–668.

Dmochowski JP, Bezdek MA, Abelson BP, Johnson JS, Schumacher EH, Parra LC. Audience preferences are predicted by temporal reliability of neural processing. *Nat Commun*. 2014:5(1):1–9.

Duan L, Zhao Z, Lin Y, Wu X, Luo Y, Xu P. Wavelet-based method for removing global physiological noise in functional near-infrared spectroscopy. *Biomed Opt Express*. 2018:9(8):3805–3820.

Erdoğan SB, Yücel MA, Akın A. Analysis of task-evoked systemic interference in fNIRS measurements: insights from fMRI. *NeuroImage*. 2014:87:490–504.

Falk E, Scholz C. Persuasion, influence, and value: perspectives from communication and social neuroscience. *Annu Rev Psychol*. 2018:69(1):329–356.

Falk EB, Berkman ET, Mann T, Harrison B, Lieberman MD. Predicting persuasion-induced behavior change from the brain. *J Neurosci*. 2010:30(25):8421–8424.

Falk EB, Berkman ET, Whalen D, Lieberman MD. Neural activity during health messaging predicts reductions in smoking above and beyond self-report. *Health Psychol*. 2011:30(2):177–185.

Falk EB, Morelli SA, Welborn BL, Dambacher K, Lieberman MD. Creating buzz: the neural correlates of effective message propagation. *Psychol Sci*. 2013:24(7):1234–1242.

Falk EB, Cascio CN, Coronel JC. Neural prediction of communication-relevant outcomes. *Commun Methods Meas*. 2015:9(1–2):30–54.

García AM, Ibáñez A. Two-person neuroscience and naturalistic social communication: the role of language and linguistic variables in brain-coupling research. *Front Psychiatry*. 2014:5:124.

Gosling SD, Rentfrow PJ, Swann WB Jr. A very brief measure of the big-five personality domains. *J Res Pers*. 2003:37(6):504–528.

Grinsted A, Moore JC, Jevrejeva S. Application of the cross wavelet transform and wavelet coherence to geophysical time series. *Nonlinear Process Geophys*. 2004:11(5/6):561–566.

Hamilton AFDC, Grafton ST. Action outcomes are represented in human inferior frontoparietal cortex. *Cereb Cortex*. 2008:18(5): 1160–1168.

Hari R, Henriksson L, Malinen S, Parkkonen L. Centrality of social interaction in human brain function. *Neuron*. 2015:88(1):181–193.

Hickok G, Poeppel D. The cortical organization of speech processing. *Nat Rev Neurosci*. 2007:8(5):393–402.

Hirsch J, Tiede M, Zhang X, Noah JA, Salama-Manteau A, Biriotti M. Interpersonal agreement and disagreement during face-to-face dialogue: an fNIRS investigation. *Front Hum Neurosci*. 2021:14:606397.

Holroyd CB. Interbrain synchrony: on wavy ground. *Trends Neurosci*. 2022:45(5):346–357.

Hoshi Y. Functional near-infrared spectroscopy: current status and future prospects. *J Biomed Opt*. 2007:12(6):062106.

Humă B, Stokoe E, Sikveland RO. Putting persuasion (back) in its interactional context. *Qual Res Psychol*. 2020:17(3):357–371.

Huppert TJ, Hoge RD, Diamond SG, Franceschini MA, Boas DA. A temporal comparison of BOLD, ASL, and NIRS hemodynamic responses to motor stimuli in adult humans. *NeuroImage*. 2006:29(2):368–382.

Iacoboni M. Imitation, empathy, and mirror neurons. *Annu Rev Psychol*. 2009:60(1):653–670.

Imhof MA, Schmälzle R, Renner B, Schupp HT. Strong health messages increase audience brain coupling. *NeuroImage*. 2020:216:16527.

Izuma K, Adolphs R. Social manipulation of preference in the human brain. *Neuron*. 2013:78(3):563–573.

Jensen B. Human reciprocity: an arctic exemplification. *Am J Orthop*. 1973:43(3):447–458.

Jiang J, Dai B, Peng D, Zhu C, Liu L, Lu C. Neural synchronization during face-to-face communication. *J Neurosci*. 2012:32(45): 16064–16069.

Jiang J, Chen C, Dai B, Shi G, Ding G, Liu L, Lu C. Leader emergence through interpersonal neural synchronization. *Proc Natl Acad Sci U S A*. 2015:112(14):4274–4279.

Jiang J, Zheng L, Lu C. A hierarchical model for interpersonal verbal communication. *Soc Cogn Affect Neurosci*. 2021:16(1–2):246–255.

Kato J, Ide H, Kabashima I, Kadota H, Takano K, Kansaku K. Neural correlates of attitude change following positive and negative advertisements. *Front Behav Neurosci*. 2009:3:6.

Keller PE, Novembre G, Hove MJ. Rhythm in joint action: psychological and neurophysiological mechanisms for real-time interpersonal coordination. *Philos Trans R Soc Lond Ser B Biol Sci*. 2014:369(1658):20130394.

Kilduff GJ, Galinsky AD. From the ephemeral to the enduring: how approach-oriented mindsets lead to greater status. *J Pers Soc Psychol*. 2013:105(5):816–831.

Kingsbury L, Huang S, Wang J, Gu K, Golshani P, Wu YE, Hong W. Correlated neural activity and encoding of behavior across brains of socially interacting animals. *Cell*. 2019:178(2): 429–446.

Kirmani A, Zhu R. Vigilant against manipulation: the effect of regulatory focus on the use of persuasion knowledge. *J Mark Res*. 2007:44(4):688–701.

Lee EJ, Shin SY. Mediated misinformation: questions answered, more questions to ask. *Am Behav Sci*. 2021:65(2):259–276.

Li R, Mayseless N, Balters S, Reiss AL. Dynamic inter-brain synchrony in reallife inter-personal cooperation: a functional near-infrared spectroscopy hyperscanning study. *Neuroimage*. 2021:238: 118263.

Li Y, Chen M, Zhang R, Li X. Experiencing happiness together facilitates dyadic coordination through the enhanced interpersonal neural synchronization. *Soc Cogn Affect Neurosci*. 2022:17(5): 447–460.

Liu J, Zhang R, Geng B, Zhang T, Yuan D, Otani S, Li X. Interplay between prior knowledge and communication mode on teaching effectiveness: interpersonal neural synchronization as a neural marker. *NeuroImage*. 2019:193:93–102.

Maris E, Oostenveld R. Nonparametric statistical testing of EEG-and MEG-data. *J Neurosci Methods*. 2007:164(1):177–190.

Matz SC, Kosinski M, Nave G, Stillwell DJ. Psychological targeting as an effective approach to digital mass persuasion. *Proc Natl Acad Sci U S A*. 2017:114(48):12714–12719.

Modic D, Anderson R, Palomäki J. We will make you like our research: the development of a susceptibility-to-persuasion scale. *PLoS One*. 2018:13(3):e0194119.

Ono Y, Zhang X, Noah JA, Dravida S, Hirsch J. Bidirectional connectivity between Broca's area and Wernicke's area during interactive verbal communication. *Brain connectivity*. 2021:12(3): 210–222.

Pan Y, Dikker S, Goldstein P, Zhu Y, Yang C, Hu Y. Instructor-learner brain coupling discriminates between instructional approaches and predicts learning. *NeuroImage*. 2020:211:116657.

Pan Y, Guyon C, Borragán G, Hu Y, Peigneux P. Interpersonal brain synchronization with instructor compensates for learner's sleep deprivation in interactive learning. *Biochem Pharmacol*. 2021:191:114111.

Pinti P, Merla A, Aichelburg C, Lind F, Power S, Swingler E, Hamilton A, Gilbert S, Burgess PW, Tachtsidis I. A novel GLM-based method for the automatic IDentification of functional events (AIDE) in fNIRS data recorded in naturalistic environments. *NeuroImage*. 2017:155:291–304.

Pinti P, Scholkmann F, Hamilton A, Burgess P, Tachtsidis I. Current status and issues regarding pre-processing of fNIRS neuroimaging data: an investigation of diverse signal filtering methods within a general linear model framework. *Front Hum Neurosci*. 2019:12:505.

Redcay E, Schilbach L. Using second-person neuroscience to elucidate the mechanisms of social interaction. *Nat Rev Neurosci*. 2019:20(8):495–505.

Reiss AL, Bryant DM, Glover GH, Liu N, Cui X. Inferring deep-brain activity from cortical activity using functional near-infrared spectroscopy. *Biomed Opt Express*. 2015:6(3):1074–1089.

Riddle PJ Jr, Newman-Norlund RD, Baer J, Thrasher JF. Neural response to pictorial health warning labels can predict smoking behavioral change. *Soc Cogn Affect Neurosci*. 2016:11(11): 1802–1811.

Rimal RN, Lapinski MK. A re-explication of social norms, ten years later. *Commun. Theory*. 2015:25:393–409.

Salazar M, Shaw DJ, Gajdoš M, Mareček R, Czekóová K, Mikl M, Brázdil M. You took the words right out of my mouth: dual-fMRI reveals intra-and inter-personal neural processes supporting verbal interaction. *NeuroImage*. 2021:228:117697.

Schippers MB, Roebroeck A, Renken R, Nanetti L, Keysers C. Mapping the information flow from one brain to another during gestural communication. *Proc Natl Acad Sci U S A*. 2010:107(20): 9388–9393.

Schmälzle R, Häcker FE, Honey CJ, Hasson U. Engaged listeners: shared neural processing of powerful political speeches. *Soc Cogn Affect Neurosci*. 2015:10(8):1137–1143.

Scholz C, Dore BP, Baek EC, O'Donnell MB, Falk EB. A neural propagation system: neurocognitive and preference synchrony in information sharers and their receivers. *Annu Meet Int Commun Assoc*. 2017.

Setlock LD, Fussell SR, Neuwirth CM. Taking it out of context: collaborating within and across cultures in face-to-face settings and via instant messaging. *Proc CSCW*. 2004:6:604–613.

Shteynberg G, Bramlett JM, Fles EH, Cameron J. The broadcast of shared attention and its impact on political persuasion. *Pers Soc Psychol*. 2016:5(5):665–673.

Simony E, Honey CJ, Chen J, Lositsky O, Yeshurun Y, Wiesel A, Hasson U. Dynamic reconfiguration of the default mode network during narrative comprehension. *Nat Commun*. 2016:7(1):1–13.

Singh AK, Okamoto M, Dan H, Jurcak V, Dan I. Spatial registration of multichannel multi-subject fNIRS data to MNI space without MRI. *NeuroImage*. 2005:27(4):842–851.

Southgate V, Begus K, Lloyd-Fox S, di Gangi V, Hamilton A. Goal representation in the infant brain. *NeuroImage*. 2014:85:294–301.

Spunt RP, Meyer ML, Lieberman MD. The default mode of human brain function primes the intentional stance. *J Cogn Neurosci*. 2015:27(6):1116–1124.

Stephens GJ, Silbert LJ, Hasson U. Speaker-listener neural coupling underlies successful communication. *Proc Natl Acad Sci U S A*. 2010:107(32):14425–14430.

Tsuzuki D, Jurcak V, Singh AK, Okamoto M, Watanabe E, Dan I. Virtual spatial registration of stand-alone fNIRS data to MNI space. *NeuroImage*. 2007:34(4):1506–1518.

Vezich IS, Katzman PL, Ames DL, Falk EB, Lieberman MD. Modulating the neural bases of persuasion: why/how, gain/loss, and users/non-users. *Soc Cogn Affect Neurosci*. 2017:12(2):283–297.

Wall HJ, Campbell CC, Kaye LK, Levy A, Bhullar N. Personality profiles and persuasion: an exploratory study investigating the role of the Big-5, type D personality and the dark triad on susceptibility to persuasion. *Pers Individ Differ*. 2019:139:69–76.

Werts CE, Linn RL, Jöreskog KG. Intraclass reliability estimates: testing structural assumptions. *Educ Psychol Meas*. 1974:34(1):25–33.

Yan C, Dillard JP, Shen F. Emotion, motivation, and the persuasive effects of message framing. *J Commun*. 2012:62(4):682–700.

Yang J, Zhang H, Ni J, De Dreu CK, Ma Y. Within-group synchronization in the prefrontal cortex associates with intergroup conflict. *Nat Neurosci*. 2020:23(6):754–760.

Zhu Y, Leong V, Hou Y, Zhang D, Pan Y, Hu Y. Instructor–learner neural synchronization during elaborated feedback predicts learning transfer. *J Edu Psychol*. 2021:114(6):1427–1441.